MODELLING OF THERMAL RADIATION AS A RESULT OF FIRES AND EXPLOSIONS FOLLOWING A WELL BLOWOUT DURING SHALE GAS PRODUCTION

Kanokwan Buaprommart, Haroun Mahgerefteh*, Sergey Martynov, Alberto Striolo

Department of Chemical Engineering, University College London, Torrington Place, London WC1E 7JE, UK

*Correspondence author: Fax: +44 20 7679 3835 Email: h.mahgerefteh@ucl.ac.uk

Keywords: thermal radiation, well blowout, shale gas production, multiphase CFD modelling

ABSTRACT

This paper presents the development and application of a multi-phase CFD flow model for predicting the thermal radiation and explosion over-pressure in the event of an accidental well blowout during shale gas production. The transient discharge rate and the fluid phase composition at the ruptured wellhead serving as the source term are determined based on the numerical solution of the conservation equations using the Method of Characteristics. Two scenarios covering immediate and delayed ignition of the escaping gas respectively leading to a jet fire or an explosion are considered. In the former case, the flow model's output, including the transient flow rate, fluid phase and composition, is linked to the widely used Chamberlain semi-empirical jet fire model to generate the resulting flame area and incident heat flux. In the case of a delayed ignition leading to an explosion, the TNO Multi-Energy Vapour Cloud Explosion is linked to the flow model to predict the resulting blast overpressure for both un-confined and partially confined explosions. The blowout model is tested by simulating the accidental well-head rupture of a real shale gas production well for which the required design, operational and prevailing ambient data are publicly available. The simulation results are presented in the form of 2D plots of thermal radiation contours as a function of distance and time and explosion overpressure/distance profiles; in turn employed to determine minimum safe distances to personnel and equipment.

NOMENCLATURE

A Flame surface area derived from flame shape (m^2)

b lift-off distance (m)

D pipe internal diameter (m)

E total specific energy (kJ/kg)

F_s fraction of the combustion energy radiated

f_w The Fanning friction factor (-)

g_x projection of the gravity force on the x axis

L_b flame length (m)

$\dot{m}$ gas discharge mass flow rate (kg/s)

p pressure (N/m^2)

P_L path length (m)

Q power radiated by the flame (kW)

q radiated flux (kW/m^2)

q_w heat flux at the pipe wall (kW/m^2)

R_H relative humidity (-)

R_L visible flame length (m)

S_{mm} saturated water vapour pressure at ambient temperature (mmHg)

S_∞ average surface emissive power (kW/ m^2)

t time (s)

T_{air} ambient temperature (K)

u velocity (m/s)

u_j gas jet velocity (m/s)

VF view factor (-)

W_1 diameter of the frustum base (m)

W_2 diameter of the frustum top (m)

x spatial coordinate along the well (m)

ρ fluid density (kg/m^3)

τ atmospheric transmissivity (-)

ΔH_c standard enthalpy of gas combustion (kJ/kg)

θ angle between release direction and vertical axis

α tilt angle of the flame

1. INTRODUCTION

The European Union currently imports ca. 50% of the natural gas it uses [1], and every year it must seek new gas contracts. Because conventional oil reserves are diminishing and renewable energy sources are in general not yet able to provide sufficient and affordable energy consistently at large

scale, shale formations have the potential of providing large sources of gas for decades to come. However, it is critically important that the design and operation of shale gas facilities meet the required safety standards for minimising or eliminating the risks to the environment and society.

Several risks are often associated with shale gas production. For example, the risk of induced seismicity caused by hydraulic fracturing has attracted wide-scale public attention [2]. Other risks exist, several of which are typical of oil and gas operations. This paper concerns the risks associated with the un-controlled release of gas, which could cause wells to blowout.

Due to the low porosity of a shale rock, parts of the formation may include gas trapped at very high pressure. Drilling into these areas may result in "pressure kicks", propagating to the wellhead and causing its blowout [3],[4]. To prevent this from happening, safety measures and devices, such as Blow-Out Preventers (BOP) are commonly used in the wells [5]. However, in the unlikely event of the failure of BOP, the resulting pressure kicks will lead to uncontrolled release of the gas and drilling mud from the formation into atmosphere [6], with the subsequent fire and explosion of the gas. Recent examples of shale well blowouts include the Acadia Parish well blowout in Louisiana [7] and the Eagle Ford well failure in Texas [8]. The Acadia Parish well blowout in Louisiana caused fire, explosion and releases of gas and salty water, resulting in evacuation of 40 residents within 1.5 miles from the well and closure of a nearby power plant [7]. In the most tragic but fortunately rare circumstances, well blowouts can result in fatalities [7], [8].

Arguably, these accidents could be prevented by following local regulations, the implementation of best practice procedures, and via the implementation of proper risk management strategies. Because Europe has a large population density, it is expected that one best practice procedure will be the reliable quantification of the minimum safe distances between drilling and production facilities and population centres, which could minimise the risks in the unlikely event of a well blowout. Such information also forms the basis for risk mitigation and emergency planning.

This paper presents the development of a failure consequence mathematical model for predicting the incident heat flux and explosion over-pressure as a result of a well blowout during shale gas production. The transient discharge rate and the fluid phase composition at the ruptured wellhead serving as the source term for the explosion and jet fire models employed are determined based on the numerical solution of the conservation equations using the Method of Characteristics [9], [10]. The flow model accounts for the important processes taking place during the depressurisation process along the well; these include real fluid behaviour, fluid/wall heat transfer and frictional effects. Based on the application of the combined well blowout model to an existing shale gas production facility, minimum safe distances are determined by reference to established thresholds for different levels of harm to people and surrounding structures.

2. METHEDOLOGY

2.1. Well discharge model

Central to the assessment of the consequences associated with a well blowout is the determination of the ensuing transient discharge rate and the fluid phase composition at the wellhead. In order to predict accurately these properties, a model is constructed accounting for all the important physical processes governing the well blowout process. In particular, to describe the transient outflow in a well, a one-dimensional model is adopted, based on the mass, momentum and energy conservation equations [11]:

$$\frac{\partial \rho}{\partial t} + \frac{\partial \rho u}{\partial x} = 0 \qquad (1)$$

$$\frac{\partial \rho u}{\partial t} + \frac{\partial \left(\rho u^2 + p \right)}{\partial x} = -\rho g_x - \frac{f_w \rho u^2}{D} \qquad (2)$$

$$\frac{\partial \rho E}{\partial t} + \frac{\partial \left(\rho u E + u p \right)}{\partial x} = -\rho u g_x - \frac{f_w \rho u^3}{D} + q_w \qquad (3)$$

where ρ, u, E and p are respectively the fluid density, velocity, total specific energy and pressure, x is the spatial coordinate along the well in the direction of discharge flow (from top to bottom), t is the time, and D is the internal diameter of the pipe running along the well. Furthermore, g_x is the local projection of the gravity force on the x axis, q_w is the heat flux at the pipe wall, and f_w is the Fanning friction factor, calculated using Chen's correlation [12]. The model accounts for variation in the inclination of the well with the depth, and can be easily extended to account for the effects of thermal and mechanical non-equilibrium between the fluid phases during the decompression process [11], as well as the variation in the flow area along the well [13]. Peng-Robinson (PR) [14] Equation of State (EoS) is employed to predict the pertinent fluid properties within the well.

To enable numerical solution of equations 1 to 3, boundary conditions are specified at the top and bottom of the well. In particular, at the bottom location, the well is assumed to be connected to an infinitely large reservoir with prescribed formation pressure. Aiming to evaluate hazardous consequences of blowout of a shale gas well for the worst-case scenarios, i.e. upon complete failure the BOP mechanism and full opening of the well to atmosphere at the ground surface, a full-bore rupture boundary condition is used at the top of the well.

Prior to the rupture, the fluid in the well is assumed to be stagnant at temperature equal to the formation temperature with the fluid pressure varying along the well according to the hydrostatic head.

The above governing equations, closed by the set of the initial and boundary conditions and the physical properties closure correlations, are solved numerically using the Method of Characteristics [15]. Natural gas from shale formations is composed of mainly methane (usually >80%) [16], mixed with ethane, propane, and butane along with smaller fractions of heavier alkanes and non-combustibles (e.g. N_2, CO_2 and H_2S). For the sake of simplicity and worst case scenario, the shale gas within the well is assumed to be pure methane.

Two failure consequences are assumed upon BOP failure; the immediate ignition of the high pressure escaping methane leading to a jet fire, and the delayed ignition resulting in an explosion.

2.2. Jet fire modelling

In order to predict the flame shape and the subsequent incident thermal radiation following the well blowout, the Chamberlain model [17], [18] for hydrocarbon fires is employed. As depicted in figure 1, the model represents the flame as a frustum of a cone, radiating as a solid body with a uniform surface emissive power. In order to determine the geometry of the flame and surface emissive power as functions of the ambient and discharge flow conditions, semi-empirical correlations are used, as described in this section.

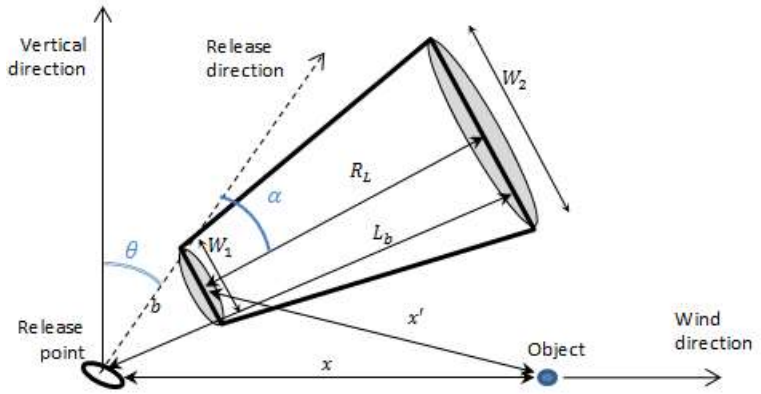

Figure 1. Schematic of the frustum of a cone representing a jet fire in Chamberlain's model [17]

2.3. Jet flame geometry

As indicated in Figure 1, the jet flame is characterised by the following set of parameters: b is the lift-off distance between the release point and the frustum base, W_1 and W_2 are the diameters of the frustum base and top faces, respectively, R_L is the visible flame length, L_b is the length of the flame measured from the release point and the tip of the flame, θ is the angle between the release direction and the vertical axis, and α is the tilt angle of the flame.

The above geometric parameters are estimated using semi-empirical correlations [17], dependent on size and orientation of the exit orifice, gas composition and wind speed including its direction and the ambient temperature. The remaining required model source terms obtained from the transient discharge model described above are the release temperature, flowrate, composition and velocity.

2.4. Surface emission model

The radiated flux at the receiver object is determined from:

$$q = \tau \times VF \times S_{\infty} \qquad (4)$$

where VF is the view factor, describing the geometric relationship between the receiver surface and the flame shape. S_{∞} is the average surface emissive power, and τ is the atmospheric transmissivity.

The average surface emissive power of the frustum, S_{∞} is calculated as:

$$S_{\infty} = \frac{F_s Q}{A} \qquad (5)$$

where A is the flame surface area derived from the flame shape, F_s is the fraction of the combustion energy radiated, and Q is power radiated by the flame. These quantities are determined using the following models.

The frustum surface area, A, is calculated knowing the diameters of the frustum at its base and the top (Figure 1):

$$A = \frac{\pi}{4}\left(W_1^2 + W_1^2\right) + \frac{\pi}{2}\left(W_1 + W_2\right)\sqrt{R_L^2 + \left(\frac{W_2 - W_1}{2}\right)^2} \qquad (6)$$

Assuming adiabatic expansion and complete combustion, the radiated power, Q, is defined as:

$$Q = \dot{m}\Delta H_c \tag{7}$$

where ΔH_c is the standard enthalpy of combustion of the gas, and $\dot{m}$ is the gas discharge mass flow rate.

For large flames F_s is approximately correlated with the gas jet velocity, u_j [17]:

$$F_s = 0.21e^{-0.00323u_j} + 0.11 \tag{8}$$

Assuming the flame black body radiation temperature of 1,500 K, and the atmospheric transmissivity is due to absorption and re-radiation by CO_2 and H_2O(g), the atmospheric transmissivity is approximated as [19, p. 50]:

$$\begin{aligned}\tau = 1.006 - 0.01171\log_{10} X_{H2O} - 0.02368\left(\log_{10} X_{H2O}\right)^2 \\ - 0.03188\log_{10} X_{CO2} + 0.001164\left(\log_{10} X_{CO2}\right)^2\end{aligned} \tag{9}$$

where

$X_{H2O} = R_H P_L S_{mm}\left(288.65/T_{air}\right)$, $X_{CO2} = P_L\left(273/T_{air}\right)$, are the mole fraction of water and the mole fraction of CO_2, respectively. R_H is the relative humidity, P_L is the path length, T_{air} is the ambient temperature and S_{mm} is the saturated water vapour pressure at the ambient temperature.

2.5. Explosion modelling

In practice, the accidental blowout of shale gas wells will result in the escape of gas into a space partially obstructed by equipment and constructions near the well pad during the drilling and fracturing operations. The delayed ignition of the release gas will lead to an explosion, creating a blast wave propagating away from the release point. The resulting explosion overpressure associated with the blast wave may pose a significant safety hazard to people and surrounding structures and should therefore be quantified as a part of the safety assessment. For this purpose, the widely established and validated TNO Multi-Energy Vapour Cloud Explosion Model [18] is employed in the present study. Linked to the transient well discharge model (section 2.1) as the source term, the model predicts the blast overpressure at various distances away from the release point at different time intervals for both un-obstructed and partially obstructed surroundings.

The peak overpressure, P_s, created by the blast wave at the ground level, is determined using empirical lookup tables provided in the TNO report [18] as a function of explosion blast strength, $P_s^{'} = P_s / P_a$, (here P_a is the atmospheric pressure) and the dimensionless radial distance to the explosion source, $r' = r\sqrt[3]{p_a / E}$, (here r and E are respectively the radial distance from the ignition source and the blast energy)

Conservatively, based on realistic tests, for unconfined vapour cloud explosions, the blast strength, $P_s^{'}$, is set to 3. In cases of partial or full confinement, the blast wave is assumed to run only in obstructed regions, where $P_s^{'}$ is set to 10 [18].

Furthermore, the blast source containing a combustible fuel-air mixture is modelled as a hemi-sphere of radius, r_o (m):

$$r_o = \frac{3E}{2\left(E_v \times \pi\right)^{1/3}} \tag{10}$$

where E_v (J/m^3) is the volumetric heat of combustion of the stoichiometric hydrocarbon-air mixture [18], and E (J) is the energy of the blast wave, defined as:

$$E = E_v V \tag{11}$$

Here V (m^3) is the volume of the cloud in specific region of interest. For fully or partially confined explosions, V is set to the volume of confinement, V_{gr} (m^3). For unconfined explosions on the other hand, V corresponds to the volume of fully expanded cloud:

$$V = V_c - V_{gr} \tag{12}$$

where V_c (m^3) is the volume of the released combustible gas cloud, which is calculated as:

$$V_c = \frac{Q_{ex}}{\rho \alpha_s} \tag{13}$$

Here ρ (kg/m^3) is the cloud density, α_s is the air-fuel stoichiometric concentration (vol%), and Q_{ex} (kg) is the amount of vapour released, as predicted using the well discharge model presented in section 2.1.

3. RESULTS AND DISCUSSION

3.1. The case study

The hypothetical blowout of the shale gas well constructed by Cuadrilla Elswick Ltd in Roseacre Wood, Lancashire, UK [20] leading to a fire (immediate ignition) or an explosion (delayed ignition) are used as a case study involving the application of the transient blowout model presented in this work. The well geometry, the site layout and meteorological data, as well as characteristics of the shale formation at various depths, have been documented in several reports [20], [21]. The relevant data required for conducting the case study failure simulation was extracted from these reports and reproduced in Table 1.

The gas pressure and temperature at the bottom of the well are prescribed based on the data reported for the Lower Bowland shale formation. In particular, the shale gas temperature is set to 343 K, while the gas pressure varies linearly between 200 bar (top of the well) and 600 bar (bottom of the well).

The surrounding air is assumed to be at 20^{o}C with a relative humidity of 50%. Based on the meteorological data [21], the wind speed at the ground surface on the site is taken as the maximum value of 10 m/s. Furthermore, the release is assumed to be vertical, while the heat exchange between the well and the formation is neglected.

Table 1. Main characteristics of the well and the reservoir conditions for fire and explosion blowout simulation

Well parameters	**Value**
Overall length	4,000 m
Material of construction	Mild steel
Wall surface roughness	0.05 mm
Heat transfer coefficient	0 W/m^2K
External diameter	127 mm
Internal diameter	114.4 mm
Wall thickness	6.2 mm
Orientation relative to horizontal	90 ^{o} (vertical)
Reservoir parameters	**Value**
Temperature	343 K
Pressure	200 bar

Application of the gas explosion model requires specification of the local level of confinement. Figure 2 shows the Rose Acre Wood site layout with four wells and drilling activities at one of the wells. The minimum area occupied by equipment near the well is *ca* 10 m^2, while the total area of the sites is *ca* 13,000 m^2. As such, for the purpose of the present study, the volume of confinement, V_{gr} , is varied in the range from 10 to 10^4 m^3.

It should be noted that to protect the site during the drilling activities, provision is made for two protection fences of 2.4 m and 4 m in height, and separated by distance *ca* 6.5 m, surrounding the site area [20]. The distance between the fences and the wells is *ca* 30 m, while the distance from the wells to the buildings within the site area varies between *ca* 40 and 80 m (figure 2). However, for the purposes of this study, a worst case scenario is assumed in which these additional barriers offer no protection against fire or explosion.

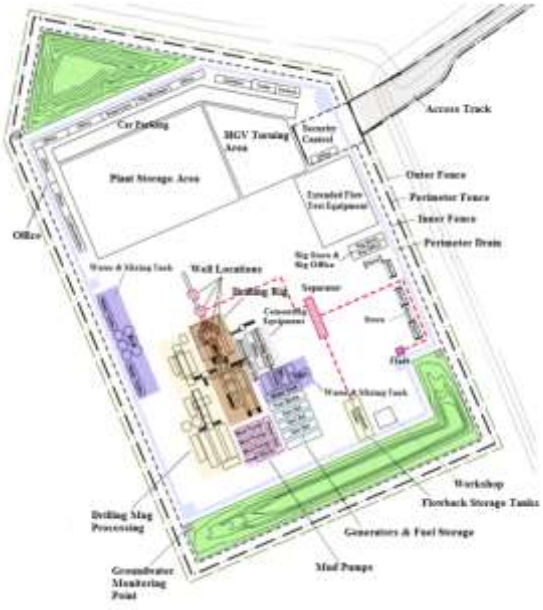

Figure 2. The layout of the Roseacre Wood well pad site for the shale gas exploration drilling and testing activities with the drilling rig surrounding one well, showing the various equipment and safeguarding fences around the site [22]. The site area is ca 100 m ×130 m.

3.2. Jet fire simulation

In the following, the simulated thermal radiation contours and safe distances for jet fires formed following accidental blowout of the shale well are presented and discussed. The failure simulations cover the well pressures of 200, 400 and 600 bar and wind speeds of 0 and 10 m/s.

Figure 3 shows the incident heat flux radiation contours at the ground level for receiver distance of +/– 200 m from the jet flame at 0.5, 2, 10 and 50 s after well blowout. The results correspond to zero wind speed and 200 bar formation pressure. As expected the incident heat flux decreases with the distance from the centre of the jet whilst decaying with time, reaching its maximum of *ca* 3 kW/m^2.

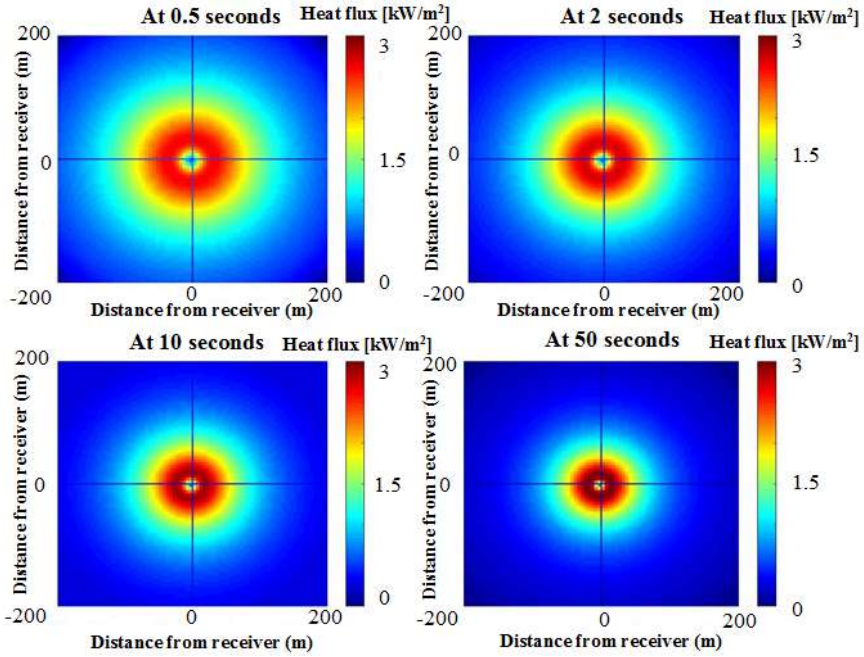

Figure 3. Incident heat flux contours at the ground level around vertical flame formed from the wellhead at (0;0), predicted at 0.5, 2, 10 and 50 s following blowout. Wind speed set to 0 m/s.

The Figure 4 shows the corresponding variation of the instantaneous incident heat flux as a function of receiver distance from the flame at different time intervals of 10 and 50 s under calm weather (no wind) and 10 m/s down-wind speed conditions. Worst case scenario is assumed in which the wind is expected to blow in the same direction as the receiver. Whilst in the time ranges investigated, the data show a small variation of heat flux with the time, the thermal radiation is a strong function of both the receiver distance and the wind speed.

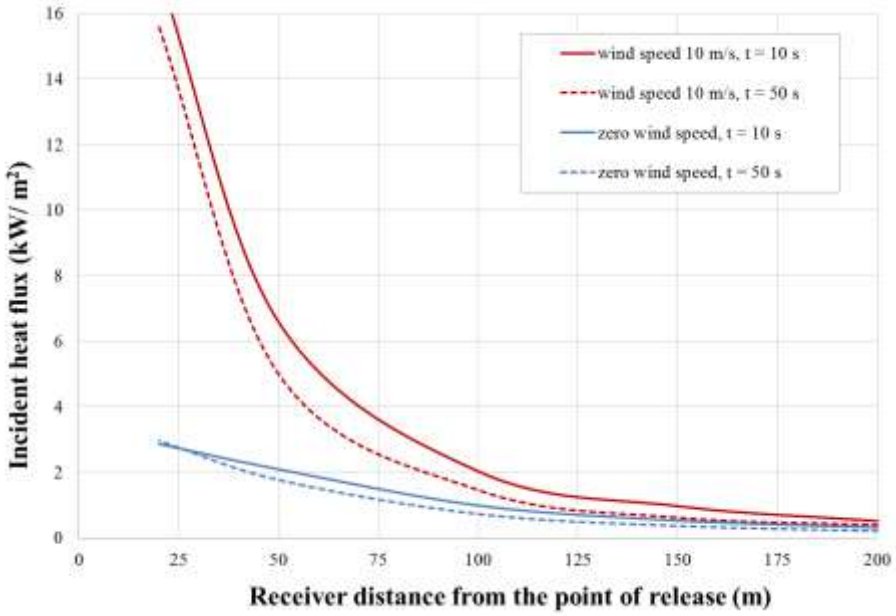

Figure 4. The incident radiation heat flux as a function of the receiver distance, predicted at 10 and 50 s during the vertical well blowout for zero and 10 m/s wind speeds.

The results in the Figure 4 followed by reference to published thermal radiation thresholds [23] may be used to determine the minimum safe distances to people and steel structures. Based on the Figure 4, at 10 s following blowout, a heat flux of 2 kW/m^2 is predicted at *ca* 50 m and 100 m from the well for zero and 10 m/s wind speeds respectively. Based on published thermal radiation thresholds data [23], exposure to this level of radiation for a period of 45 s may result in severe pain, while exposure exceeding 187 s may cause second degree burn.

Figure 5 shows the simulated variations of the minimum safe distances to personnel (6.3 kW/m^2 threshold) and steel structures (35 kW/m^2 threshold) for jet fires formed following well blowout for methane formation pressures of 200, 400 and 600 bar. A wind speed of 10 m/s is assumed.

As it may be observed, at all times the safe distances to personnel are nearly 2 to 2.5 times larger than those required for the steel structures. Also, at any given formation pressure, the minimum safe distance initially rapidly decreases with time upon blowout, consistent with an initial rapid depressurisation. This trend is next followed by a much less marked reduction in the minimum safe distance as the well gradually depressurises.

Longest safe distances in the Figure 5 are predicted at the moment of release where the discharge rate and the flame length are at their peak values. Based on this scenario, the minimum estimated worst case safe distance for personnel is *ca* 140 m, while that for steel structures is 40 m away from the well.

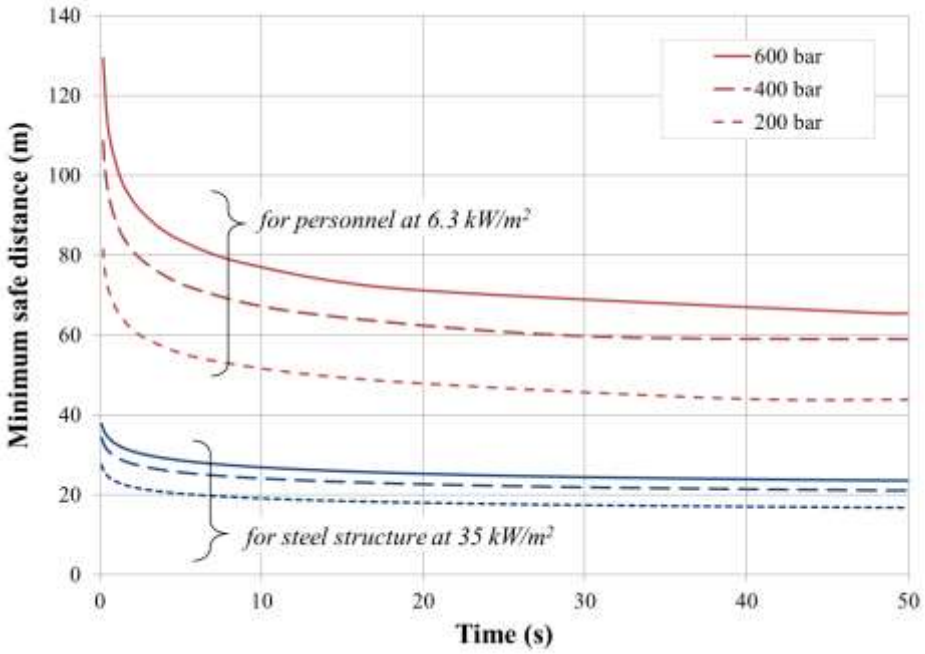

Figure 5. Safe distances to a vertical flame for personnel (outside the buildings and unprotected) and steel structures, calculated for 200, 400 and 600 bar formation pressures for natural gas containing 100 mol% of methane. Wind speed 10 m/s. The terrain is assumed to be flat with no firewalls in place.

3.3. Explosion simulation

In the following, the results of simulations of blast overpressures are presented and discussed in the context of safe distances for personnel working at the well site. Given that the site equipment and facilities represent partial obstruction to the explosion, to account for these, the volume of confinement, V_{gr}, is varied between 10 and 10,000 m^3 representative of one-storey buildings (3 m high) with the length ranging from *ca* 2 to 55 m.

For the sake of example, the results are obtained for 200 bar formation pressure. Following TNO recommendation [18], the blast strengths were respectively set to 3 bar and 10 bar for explosions in unconfined and partially spaces. An arbitrarily ignition delay of 1 s following a well blowout is assumed.

Figure 6 shows the predicted variation of peak overpressure as a function of distance from the explosion source located at the wellhead following well blowout. The results are plotted for various volumes of confinement, V_{gr} in the range from 0 to 10^4 m^3. The two hazardous overpressure thresholds of 70 mbar 300 mbar relevant to different types of injures to personnel working in open space areas and in buildings are also indicated in the same figure as examples.

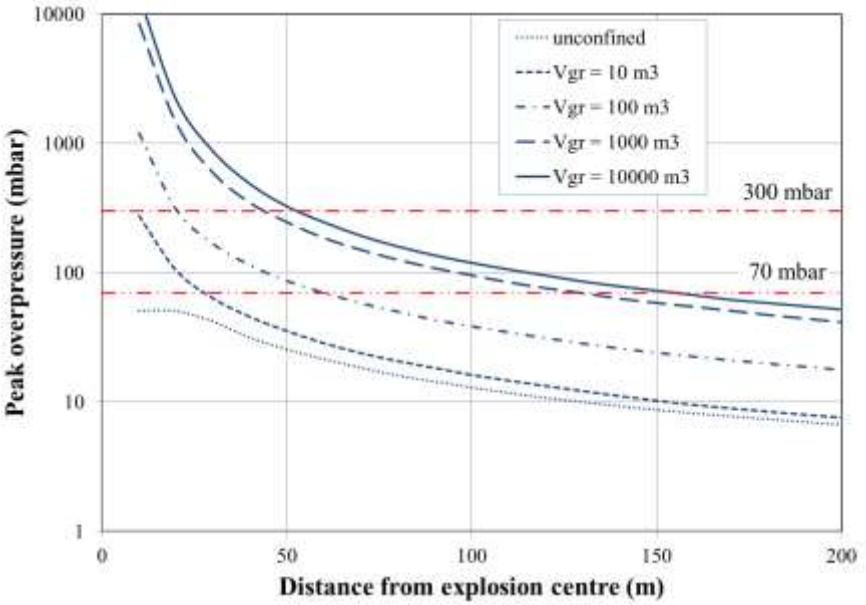

Figure 6. Explosion overpressure as a function of distance from the explosion source for various levels of confinement.

Table 2. Potential damage and fatalities peak overpressure thresholds for people working in different types of buildings [23].

Type of location	**Peak overpressure (mbar)**	**Potential damage**
People in the open	300	Eardrum rupture
	1000	Picked up and thrown; likely fatality
People in normal buildings	70 - 250	Significant likelihood of fatality due to masonry collapse and projectiles, particularly glass
Blast resistant buildings	> 200	Some likely fatality
Blast proof buildings	> 1000	Some likely fatality

Table 2 shows peak overpressures corresponding to various types of injuries for people working in different types of locations in the event of a vapour cloud explosion [23]. The results in Figure 6 show that explosion overpressures above 300 mbar can be expected to be within ca 10 m to 50 m radius from the explosion centre for confinement volumes between 10 and 10,000 m^3 respectively.

For people inside normal buildings, Table 2 suggests 70 mbar as potentially fatal overpressure threshold. From Figure 6 it can be seen that overpressures above 70 mbar can be expected within ca 150 m radius from the explosion centre for highly obstructed regions (V_{gr} = 10,000 m^3) and less than 60 m for low-obstructed regions (V_{gr} = 100 m^3).

As such, the simulated overpressure data indicate no risk of fatalities for people in normal buildings located at more than 60 m away from an explosion originating at the drilling pad. In this case, the maximum predicted explosion overpressure falls below the 70 mbar threshold needed to cause a fatality. This finding is consistent with the plant layout, where offices, stores, workshop and laboratories are placed at more than 50 m away from the wells.

CONCLUSIONS

This paper described the development and application of a transient computationally based fluid flow model linked to established empirically based jet fire and explosion correlations for determining the minimum safe distances to personnel and steel structures in the event of a well head blowout during shale gas production.

The model's testing is based on its application to a hypothetical scenarios involving well blowout at the Rose Acre shale gas exploration site in the UK during the drilling stage. The simulation results are presented in the form of 2D plots of thermal radiation contours as a function of distance and time and explosion over-pressure/distance profiles for an arbitrary 1 s delay in the detonation of the released gas from the wellhead.

Parametric studies are conducted in order to demonstrate the impact of changes in the formation pressure and wind speed on the resulting jet fire incident heat flux and explosion over-pressure, the latter for different degrees of confinement.

The minimum distances coinciding with various degrees of harm including 2nd degree burns, explosion injuries or fatalities are determined by reference to the relevant published fire and explosion harm thresholds.

For the case study considered, the results indicate that jet fire consequences are minimal for personnel working outside buildings located at distances of more than 100 m away from the wellhead.

The well blowout simulation study indicates that fire and explosion hazard consequences are minimal for personnel working in buildings located at distances of more than 60 m away from the wellheads. These findings are qualitatively consistent with layout of the Rose Acre Wood shale gas site where the buildings are sited over 60 m away from the wellhead.

In conclusion, the modelling and the methodology presented in this report is shown to serve as a useful tool for quantitative risk assessment of shale gas facilities, to ensure safe design layout and thereby minimising the consequences of a well blowout.

ACKNOWLEDGMENTS

This work has received funding from the European Union's Horizon 2020 research and innovation programme under grant agreement no. 640979. The work reflects only the authors' views and the European Union is not liable for any use that may be made of the information contained therein.

REFERENCES

[1] Comissão Europeia, "Imports and secure supplies - European Commission," 2017. [Online] Available: https://ec.europa.eu/energy/en/topics/imports-and-secure-supplies. [Accessed: 18

August 2018]
[2] R. Davies, G. Foulger, A. Bindley, and P. Styles, “Induced seismicity and hydraulic fracturing for the recovery of hydrocarbons,” *Mar. Pet. Geol.*, vol. 45, pp. 171–185, Aug. 2013.
[3] S. Willson, “A Wellbore Stability Approach For Self-Killing Blowout Assessment,” *SPE Deep. Drill. Complet. Conf.*, Texas, USA, 2012 , pp. 20–21.
[4] I. Duncan, “Likelihood and Environmental Consequences of Blowouts of Shale Gas and Shale Oil Wells,” pp. 9–11, 2016.
[5] P. Skalle, *Pressure Control During Oil Well Drilling*, 6th ed. bookboon, 2015.
[6] J. Boak, “Chapter 6. Shale-Hosted Hydrocarbons and Hydraulic Fracturing,” in *Future Energy*, T. M. Letcher, 2nd ed. Elsevier Ltd, 2014.
[7] KLFY.com, “No injuries in well blowout in Acadia Parish,” 2017. [Online] Available: http://kpel965.com/no-injuries-in-well-blowout-in-acadia-parish/ [Accessed: 20 July 2018].
[8] R. T. Dukes, “Eagle Ford Well Blowout Near Petersville - EOG & Nabors,” 2017. [Online] Available: https://eaglefordshale.com/efs-news/news/eagle-ford-well-blowout-near-petersville-eog-nabors [Accessed: 25 July 2018].
[9] M. J. Zucrow and J.D. Hoffman, *Gas dynamics*, New York: Wiley, 1976.
[10] H. Mahgerefteh, A. O. Oke, and Y. Rykov, “Efficient numerical solution for highly transient flows,” *Chem. Eng. Sci.*, vol. 61, no. 15, pp. 5049–5056, 2006.
[11] S. Brown, S. Martynov, H. Mahgerefteh, and C. Proust, “A homogeneous relaxation flow model for the full bore rupture of dense phase CO_2 pipelines,” *Int. J. Greenh. Gas Control*, vol. 17, pp. 349–356, Sep. 2013.
[12] N. H. Chen, “An Explicit Equation for Friction Factor in Pipe,” *Ind. Eng. Chem. Fundam.*, vol. 18, no. 3, pp. 296–297, Aug. 1979.
[13] S. Brown, S. Martynov, and H. Mahgerefeth, “Simulation of two-phase flow through ducts with discontinuous cross-section,” *Comput. Fluids*, 2015.
[14] D. Wu and S. Chen, “A Modified Peng-Robinson Equation of State,” *Chem. Eng. Commun.*, vol. 156, no. 1, pp. 215–225, Feb. 1997.
[15] E. F. Toro, “The HLL and HLLC Riemann Solvers,” in *Riemann Solvers and Numerical Methods for Fluid Dynamics*, 1997, pp. 293–311.
[16] L. Stamford and A. Azapagic, “Life cycle environmental impacts of UK shale gas,” *Appl. Energy*, vol. 134, pp. 506–518, 2014.
[17] G. A. Chamberlain, “Developments in Design Methods for Predicting Thermal Radiation From Flares,” *Chem. Eng. Res. Des.*, vol. 65, no. July 1987, pp. 299–309, 1987.
[18] TNO, *Methods for the Calculation of Physical Effects*, 3rd Ed., The Hague: TNO, 2005.
[19] L. Phillips, *Shell FRED Technical Guide*, no. 5.0. Chester, England: Shell Research Ltd., 2007.
[20] Cuadrilla Elswick Ltd, “Exploration Works Planning Application,” Cuadrilla Elswick Ltd., Lancashire., United Kingdom, June, 2014.
[21] Cuadrilla Elswick Ltd, “Environmental Statement,” Cuadrilla Elswick Ltd., Lancashire., United Kingdom, June, 2014.
[22] F. Egan, “Emerging findings of the environmental impact assessment: Roseacre Wood,” Cuadrilla Elswick Ltd, Lancashire., United Kingdom, June, 2014.
[23] DOT, *Handbook of Chemical Hazard Analysis Procedures. Federal Emergency Management Agency, U.S. Department of Transportation, and U.S. Environmental Protection Agency.* Washington, D.C.: Federal Emergency Management Agency Publications Office, 1988.